Quantifiable fluorescent glycan microarrays

**Xuezheng Song · Baoyun Xia · Yi Lasanajak ·
David F. Smith · Richard D. Cummings**

Abstract A glycan microarray was developed by using 2,6-diaminopyridine (DAP) as a fluorescent linker and printing of the glycan-DAP conjugates (GDAPs) on epoxy-activated glass slides. Importantly, all coupled GDAPs showed a detectable level of concentration-dependent GDAP fluorescence under blue laser excitation (495 nm) that can be used for both grid location and on-slide quantification. A glycan array including a large number of GDAP's derived from natural and commercially available free glycans was constructed and glycan interactions with various plant lectins were investigated. In addition, binding parameters of lectins to glycans were obtained by varying both the amount of GDAPs on the array and the lectin concentration in analyses. These data demonstrate the general utility of GDAP microarrays for functional glycomic analyses and for determining binding parameters of glycan binding proteins (GBPs).

Keywords Carbohydrate · Glycan conjugate · Glycomics · Microarray · Fluorescence

Abbreviations

DAP	2,6-diaminopyridine
GDAP	glycan-DAP conjugate
HPLC	high performance liquid chromatography
NHS	N-hydroxysuccinimde
RFU	relative fluorescence unit
GBP	glycan binding protein
RCA I	*Ricinus communis* agglutinin I
AAL	*Aleuria aurantia* lectin
ConA	concanavalin A
SNA	*Sambucus nigra* agglutinin
LTL	*Lotus tetragonolobus* lectin
LNnH	lacto-*N*-neohexaose
LNFIII	lacto-*N*-fucopentaose III
FITC	fluorescein isothiocyanate

X. Song · B. Xia · Y. Lasanajak · D. F. Smith ·
R. D. Cummings (✉)
Department of Biochemistry,
Emory University School of Medicine,
O. Wayne Rollins Research Center, 1510 Clifton Road,
Suite 4001,
Atlanta, GA 30322, USA
e-mail: rdcummi@emory.edu

Introduction

Complex carbohydrates are among the most important biomolecules, however, studies of their molecular interactions have lagged behind studies of other important macromolecules, such as nucleic acids and proteins. Glycan components of glycoproteins, glycolipids, and proteoglycans have complex and often branched structures and historically they have been difficult to synthesize and analyze [22]. An outgrowth of interest in glycan function has been termed functional glycomics, which focuses on the nature of glycan interaction with glycan binding proteins [2, 7]. Such interactions are important in cell adhesion, cell signaling, and other biological pathways and therefore considered important targets of biomedical research [10, 13, 17].

A key new development in the area of functional glycomics has been glycan microarrays, in which glycans are either covalently or non-covalently immobilized on glass slides for investigating the specificity of glycan-binding proteins (GBPs) [2, 3, 5, 8, 11, 18, 23]. A widely available large-scale glycan microarray employs *N*-hydroxysuccinimide (NHS)-activated glass slides that are

chemically reacted with glycans containing an aliphatic amine spacer at their reducing end [2]. While this approach is highly successful, it is limited so far by the need to chemically synthesize glycans with the amine spacer.

We previously described the preparation of glycan derivatives by reductive amination with 2,6-diaminopyridine (DAP) to generate glycan-DAPs (GDAPs) that provide a reactive amino group for coupling to amine-reactive solid substrates [25]. A key feature of this approach is that the GDAPs are fluorescent and permit micro-scale preparations of glycans that facilitate glycan purification and quantification. Initial studies of such GDAP derivatives indicated their successful printing on NHS-activated glass slides [25], but the utility of such printing was questioned in a recent study comparing GDAP derivatives to glycans derivatized with an alternative bifunctional spacer [3]. Here we report the production of glycan microarrays using GDAP derivatives on amine-reactive glass surfaces where we have compared printing on NHS- vs epoxy-activated glass slides. We demonstrate the utility of GDAPs for quantifying glycans printed on an epoxy-activated slide using piezoelectric printing techniques and intrinsic fluorescence of the GDAPs on the array. This novel methodology provides an excellent platform for natural glycan array development by facilitating the separation and immobilization of small amount of glycans from natural sources.

Results

### The fluorescence property of glycan-DAP conjugates

The general scheme for generating a natural glycan array with free, reducing glycans conjugated with DAP is illustrated in Fig. 1. The resulting mixture of GDAPs may be separated by HPLC using the fluorescence of the DAP functional group (excitation at 330 nm and emission at 400 nm) for detection. The separated glycans may be subsequently printed on activated glass slides, such as NHS-activated or epoxy-activated slides. In our preliminary experiments, we compared the printing behavior of GDAPs on NHS-slides vs epoxy slides, as shown in Fig. 2 using LFNIII-DAP. Immobilized LNFIII-DAP was incubated with biotinylated *Aleuria aurantia* lectin (AAL), which was detected by incubation with cyanine-5 streptavidin. AAL is a tetrameric and tetravalent mushroom lectin that binds with high degree of specificity to α-fucose-containing glycans [12, 27]. On NHS slides, clear signals were obtained from the AAL binding when the printing concentration of LNFIII-DAP was above 16 μM. On epoxy-activated slides, an even lower concentration was detectable at 4 μM. Because of the higher sensitivity and relatively uniform spot size and morphology we utilized epoxy slides for all further studies. These data show that LNFIII-DAP can be efficiently printed with good sensitivity and detectability on both NHS and epoxy slides, which stands in sharp contrast to a recent report where printing of a single GDAP (LNnT-DAP) on NHS slides was poorly detectable by the plant lectin RCA-I at even higher concentrations of printed glycan [3]. This discrepancy may be due to the relatively low affinity of RCA-I for LNnT under the assay conditions used.

When the GDAP reacts with the epoxy glass surface, the fluorophore is structurally modified. It was necessary, therefore, to evaluate the fluorescence properties of GDAPs after reaction with amino-reactive glass surface. To evaluate and quantify GDAP-glycan during the HPLC separation and after they are printed on glass slides, we prepared standards containing the relevant fluorophores, namely, lactose-DAP conjugate (Lac-DAP) and lactose-DAP-lactose double conjugate (Lac-DAP-Lac or L-DAP-L) (Fig. 3).

Lac-DAP can be used as a standard to quantify different GDAPs during their HPLC separation, while Lac-DAP-Lac, which is structurally similar to the GDAPs after they react with epoxy, can be used for the "on-slide" quantifi-

Fig. 1 The principle of the natural glycan array using DAP as a fluorescent linker. Reducing glycans from natural sources are reductively aminated to form fluorescent glycan derivatives suitable for monitoring and HPLC separation. The separated GDAPs can be covalently attached to activated surfaces to form a glycan microarray
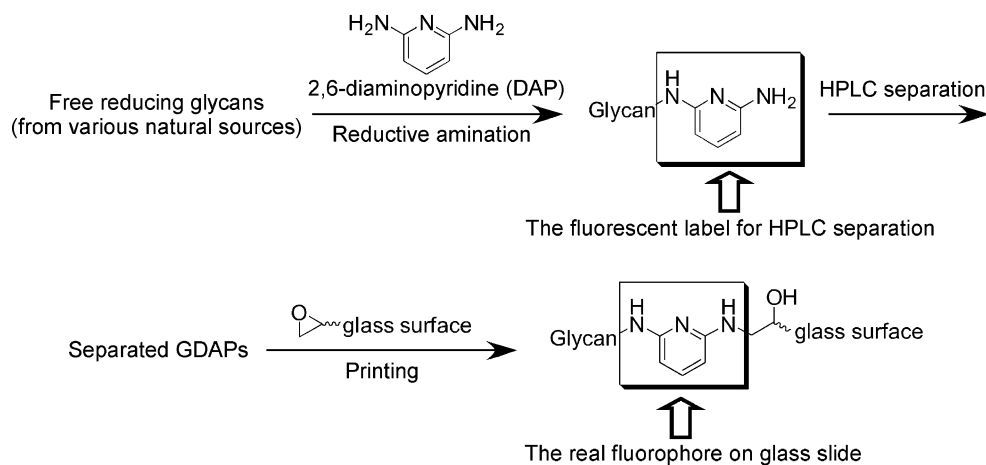
Fig. 2 The comparison of LNFIII-DAP printed on NHS slide and epoxy slide. LNFIII-DAP, LNFIII and DAP (concentration from 1 mM to 0.1 µM by twofold serial dilution in 300 mM phosphate buffer, pH 8.5) were printed on both **a** NHS slide and **b** epoxy slide. After blocking, the slides were incubated with 1 µg/ml AAL, which was detected by 5 µg/ml cyanine-5 streptavidin
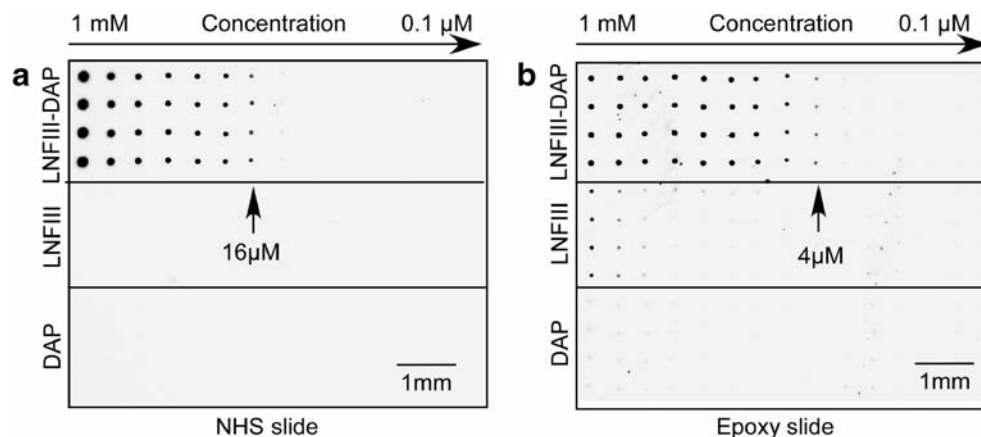
cation standard. The HPLC profiles of 20 pmol of DAP, Lac-DAP and Lac-DAP-Lac are shown in Fig. 3b, using 330 nm excitation and 400 nm emission, which are the optimal excitation and emission wavelengths of GDAP [25]. Under optimal conditions the GDAP derivatives show clear fluorescence emission of similar intensity at the pmol level; therefore, GDAPs of glycans released from a natural source can be quantified during HPLC separation using either fluorescence or UV absorption. The on-slide quantification of GDAPs is restricted by the limitation of the microarray scanner, which is equipped with four lasers covering an excitation wavelength range from 488 to 649 nm. The shortest excitation wavelength, 488 nm, is far from the optimal 330 nm excitation wavelength of the GDAPs. Nevertheless, we explored the possibility of fluorescence-based, on-slide spot localization and quantification. We evaluated the fluorescence property of Lac-DAP

and Lac-DAP-Lac at 495 nm excitation and 520 nm emission (the standard setting for Alexa488 fluorescence), including the HPLC profiles of 20 nmol DAP, Lac-DAP and Lac-DAP-Lac (Fig. 3c). The fluorescence at the excitation wavelength of 495 nm is about 10^4-fold weaker compared to that at 300 nm excitation wavelength, but we observed a stronger fluorescence from Lac-DAP-Lac compared to either DAP or Lac-DAP. These results show that after the primary amine is N-alkylated, its fluorescence at this excitation wavelength increases. This weak but measurable fluorescence at an excitation wavelength of 495 nm encouraged us to explore the possibility of on-slide quantification of glycans.

Our preliminary experiments showed that the PBS buffer (pH 7.4) is a suitable printing buffer for epoxy slides, and it was therefore used in our printing throughout this study. DAP, Lac-DAP, Lac-DAP-Lac and a blank buffer control

Fig. 3 The fluorescence properties of DAP and DAP conjugates. **a** Preparation of Lac-DAP and Lac-DAP-Lac as quantification standards of GDAPs; **b** HPLC profiles of DAP, Lac-DAP and Lac-DAP-Lac using fluorescence detection at 330 nm (Ex) and 400 nm (Em); 20pmol of each compound was injected; **c** HPLC profiles of DAP, Lac-DAP and Lac-DAP-Lac using fluorescence detection at 495 nm (Ex) and 520 nm (Em); 20 nmol of each compound was injected
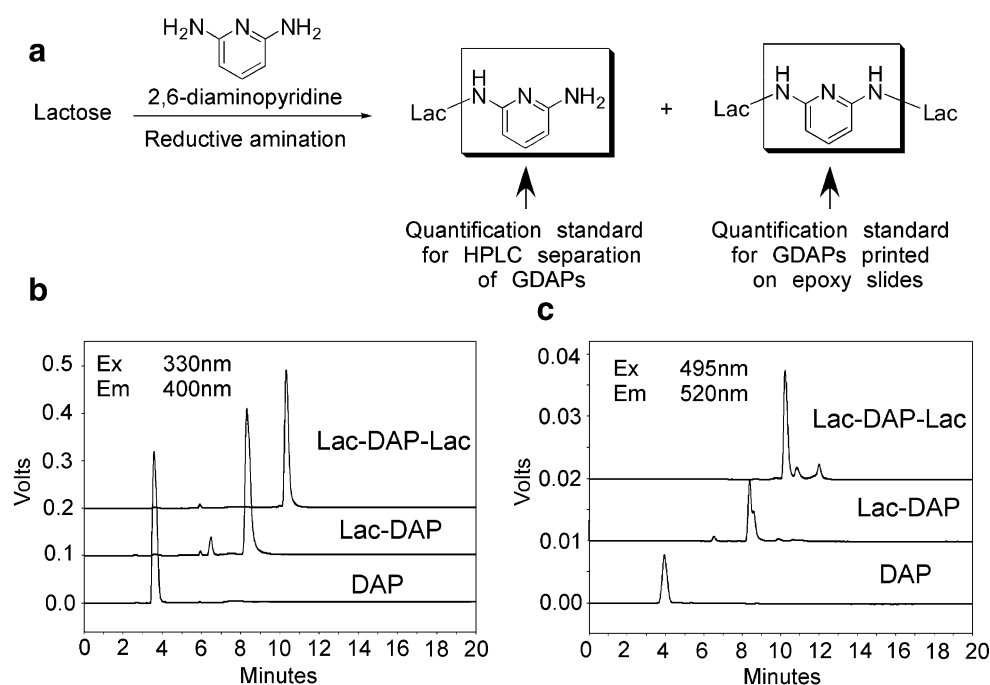
were printed on an epoxy glass slide, and immediately after printing, the slide was scanned at 495 nm excitation with 520 nm emission (Fig. 4a). The deposited material has a reflection signal as a background, but after washing the reflection signal is lost (compare the spots of the PBS replicates in Fig. 4a to those in Fig. 4b). Compared to the reflection signal from the negative control, in which only blank buffer was printed, we observed clear fluorescent signals for DAP, Lac-DAP and Lac-DAP-Lac. The linear relationship between the fluorescence of Lac-DAP-Lac and the printing concentrations (Fig. 4a) indicates that this analysis may be used as the on-slide quantification standard. After incubation at 50°C in a humidified chamber for 12 h, the slide was blocked by 50 mM ethanolamine in 0.1 M Tris buffer (pH 9.0), washed with deionized water, dried by centrifuging in a slide centrifuge for 30 s (or with a gentle stream of N_2) and scanned again using the same fluorescence setting (Fig. 4b). Since Lac-DAP-Lac has no primary amine functional group, it was largely removed after washing from the epoxy-derivatized surface; therefore, it showed much lower fluorescence compared to that before blocking. Some residual attachment of the LNFPIII may be due to the reactivity of epoxy functional groups with hydroxyls at high concentrations, as described below. As would be expected, DAP reacted with the epoxy surface effectively, as shown by the fluorescence after washing and blocking (Fig. 4b). More importantly, the covalently-coupled Lac-DAP generated a fluorophore (Lac-DAP-glass), which is structurally similar to Lac-DAP-Lac, and which has stronger fluorescence than Lac-DAP itself. Consequently, after blocking, Lac-DAP derivatized to glass

showed an "on-slide" fluorescence, which could be used to quantify Lac-DAP using Lac-DAP-Lac as a standard. The linear relationship between the fluorescence of Lac-DAP-glass and the original printing concentration suggested a relatively stable printing efficiency within this concentration range. The slope of Lac-DAP-glass vs printing concentration (Fig. 4b) was lower than the slope of Lac-DAP-Lac vs printing concentration (Fig. 4a); presumably due to the loss of Lac-DAP after blocking, which reflects the amount covalently coupled. The ratio of the slope from Fig. 4b to the slope from Fig. 4a (approximately 44%) probably represents a reasonable estimate of the average yield of Lac-DAP immobilized on epoxy glass slides under these printing conditions. Using this approach, we established that different GDAPs are printed on epoxy-activated glass slides with efficiency in the range of 30–45%. This efficiency is similar to that obtained for oligonucleotide printing on epoxy-activated glass slides [14, 20].

A microarray of glycan-DAP conjugates

With the success of being able to visualize the printed GDAPs directly and define the efficiency of printing, we explored the use of these derivatives in a glycan microarray format. We generated a glycan microarray of 21 GDAPs prepared from free, reducing glycans that are listed in Table 1. The overall layout of the glycan array of GDAPs, which included six replicated subarrays, is shown in Fig. 5a. All the GDAPs were printed at 200 μM. This concentration is in the general range of that used by the Consortium for Functional Glycomics, where the glycan

Fig. 4 The printing of DAP, Lac-DAP and Lac-DAP-Lac on epoxy slides. **a** DAP, Lac-DAP, Lac-DAP-Lac scanned at Alexa488 setting (Ex 495 nm, Em 520 nm) immediately after printed on epoxy glass slides (in PBS 7.4 buffer). The concentration dependence of the relative fluorescence unit (RFU) of Lac-DAP-Lac was fitted linearly. **b** The slide was incubated at 50°C moisture chamber, blocked and scanned at Alexa488. The concentration dependence of the relative fluorescence unit (RFU) of Lac-DAP-glass was fitted linearly

$y = 22.153x + 1165.7$
$R^2 = 0.9872$

$y = 9.7836x + 1155.8$
$R^2 = 0.9605$
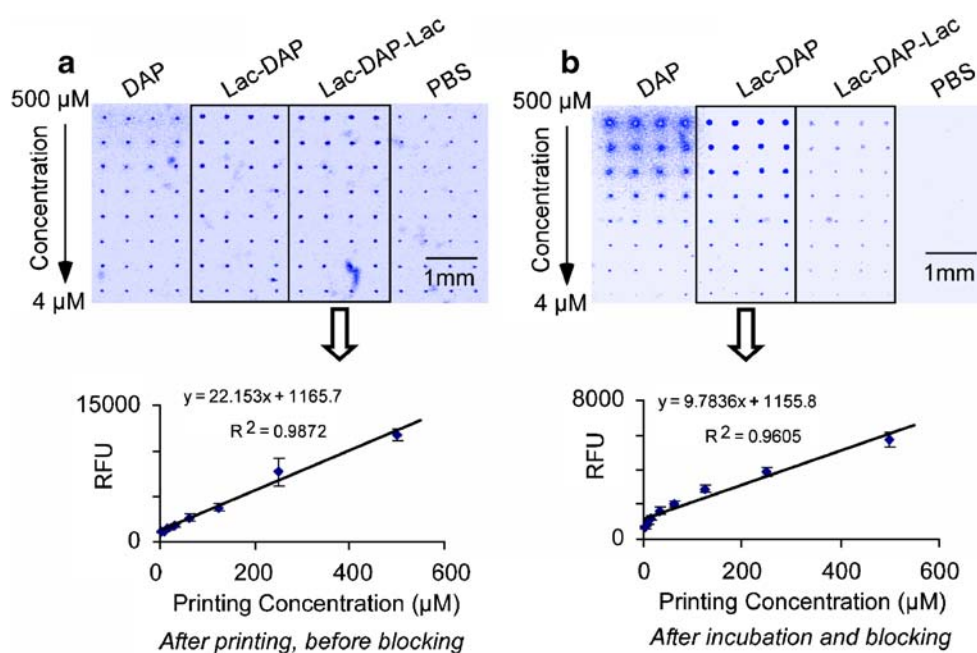
Table 1 Structures and designations of glycans used in this study
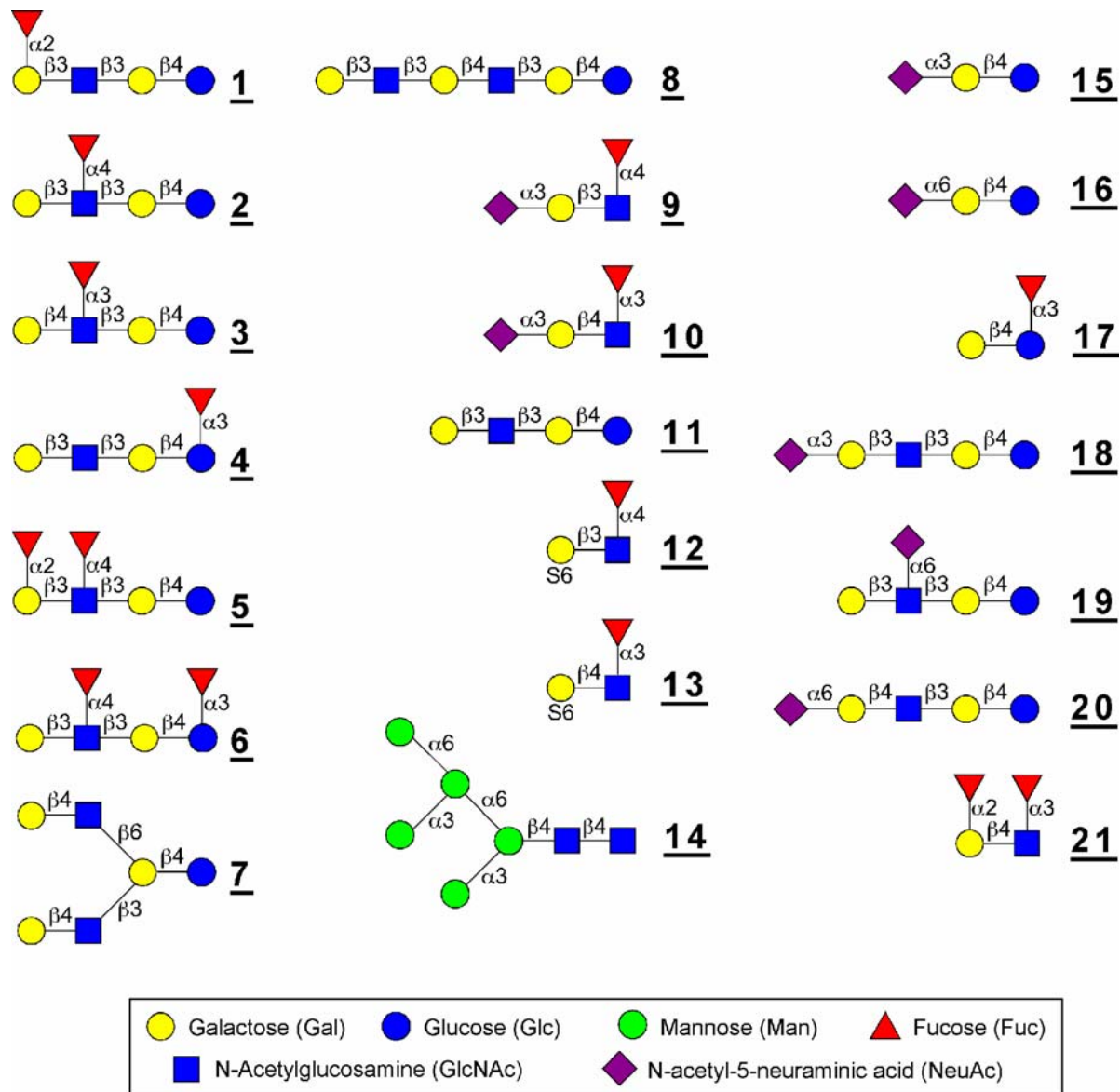
Fig. 5 A glycan array of 21 GDAPs. All samples are printed at 200 μM. **a** The overall layout. The microarray includes 6 replicated subarrays. In each subarray, 21 GDAPs (16 replica) and 3 controls (DAP, PBS buffer, lactose) are printed. **b** A subarray after printing, incubation at 50°C moisture chamber for 12 h, followed by blocking. The slide was scanned with fluorescence detection at 495 nm (Ex) and 520 nm (Em). The grid can be easily located by the fluorescence of the GDAPs
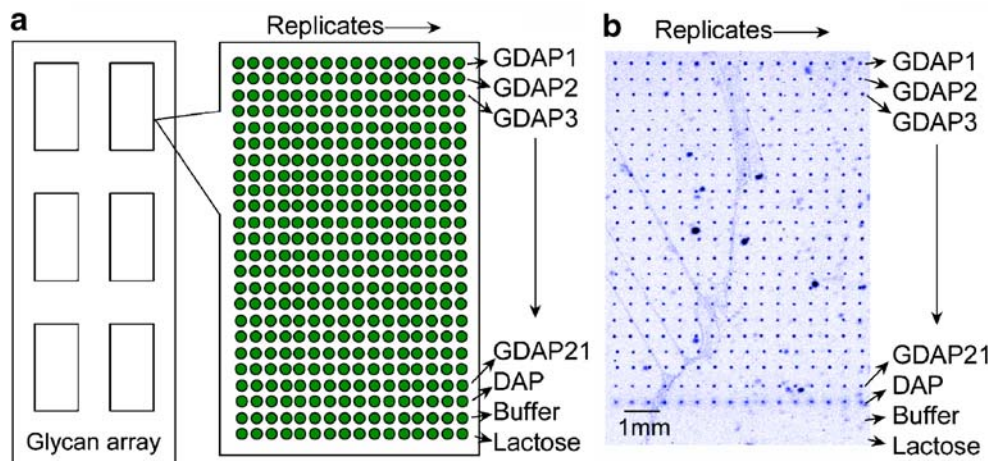
microarray is printed at 100 μM [2]. In each subarray the GDAPs (16 replicates) and three controls (DAP, PBS, lactose) were printed. After incubation and blocking, the microarray was scanned at excitation of 495 nm with emission at 520 nm.

The fluorescence image of a single subarray after printing and blocking is shown in Fig. 5b. Other than blank buffer and lactose solution, all the samples with the DAP functional group showed clear, low level fluorescence. This fluorescence allowed us to create an image of the grid location for each glycan and also served as a quality control measure to ensure that each of the GDAPs was printed appropriately and at equivalent densities. Since grid localization is sometimes difficult to achieve and quantification on the microarray is not possible with other

prevailing linking strategies, this is a significant advantage of the GDAP method for glycan microarrays.

This glycan microarray was explored with various biotinylated lectins, which were detected with cyanine-5 streptavidin by a second incubation. The binding results are shown in Fig. 6. We explored the binding of RCA-I (terminal galactosides), AAL (terminal α-fucosides), Con A (oligomannose-, hybrid-, and complex-type biantennary N-glycans), *Sambucus nigra* agglutinin (SNA) (terminal α6-sialosides), and *Lotus tetragonolobus* lectin (LTL) (terminal α3-fucosides, including Lewis x-type structures) [4, 15, 26]. All the lectins showed expected binding to the sugar structures on the GDAP microarray with high specificity (Fig. 6). The typical signal/noise in these analyses was excellent and clear binding above background was ob-

Fig. 6 The binding assay of various lectins to GDAPs on the microarray. Biotinylated lectins were detected with cyanine-5 streptavidin by a second incubation. The microarray was scanned at 649 nm excitation and 670 nm emission. The images are shown in *red*. For every image, a histogram was generated for easy analysis. a AAL binding to fucose-contained glycans; b SNA binding to 6-sialylated LacNAc; c Con A binding to oligomannose5; d RCA I binding to LNnH; e LTL binding to Galβ1–4(Fucα1–3)GlcNAc and Galβ1–4(Fucα1–3)Glc
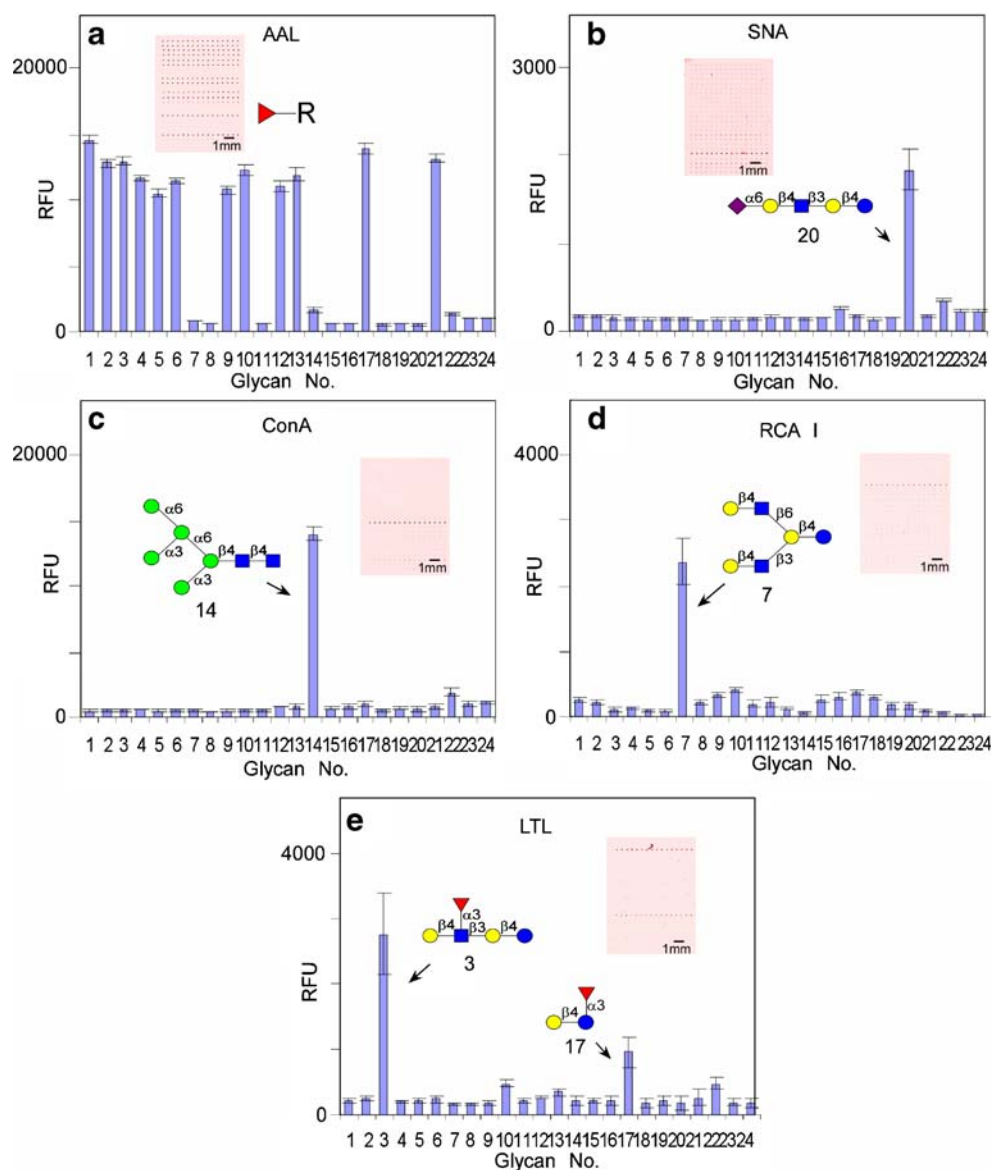
served. These results demonstrate the utility of GDAP microarray for evaluating the specificity of GBPs.

A binding study of LNFIII-AAL on the microarray

Glycan microarrays have been most commonly used as a screening tool for protein–carbohydrate interactions. The inability to detect derivatized glycans directly on the slide prior to any analysis has been a barrier to using glycan microarray for more detailed binding study between glycans and glycan binding proteins and microorganisms. Most binding studies using glycan microarrays are based on printing with defined concentrations of glycan derivatives assuming saturation of available coupling or a high printing efficiency of coupling after printing. With the GDAP microarray, however, it is possible to directly quantify glycans on the microarray, thus permitting more detailed binding assays where protein or organism bound to the array can be quantified as a function of actual amount of glycan on the printed surface.

We chose to explore the specific binding of AAL to LNFIII as a model system based on the previous screening of various lectins on the GDAP microarray (Fig. 6). A microarray of a single GDAP (LNFIII-DAP) was printed at different glycan concentrations from 1 μM to 10 mM, blocked as described above. The results in Fig. 7a show the image scanned at excitation 495 nm with emission at 520 nm after blocking. The corresponding charts below the images show the relationship between the RFU and printing concentration. We observed that at printing concentrations above 1 mM, the printing efficiency was reduced, probably due to the saturation of the active epoxy groups on the slide by LNFIII-DAP. The saturation of surface active groups is an expected problem when the printing concentrations are relatively high. Under this condition, the direct on-slide quantification becomes very important to avoid any misinterpretation of binding assay data based on the original printing concentration. Based on the GDAP fluorescence, the actual amount of LNFIII-DAP immobilized on the slides can be easily calculated using the Lac-DAP-Lac standard curve (Fig. 4). These conveniently calculated on-slide values (fmol/spot) were then used in the data analysis after the lectin binding assay. The image of the array after being assayed with AAL at 20 μg/ml is shown in Fig. 7b. The RFU of AAL binding has a linear relationship with the actual on-slide concentration of LNFIII-DAP, as shown in the fitted curve. The intrinsic fluorescence of the GDAP on the microarray has no

Fig. 7 Various concentrations of LNFIII-DAP were printed on epoxy slide. a After printing and blocking, the GDAP fluorescence was measured. The printing efficiency drops quickly at higher concentrations. b The slide was assayed with AAL (20 μg/ml) and stained with cyanine-5 streptavidin. The fluorescence was drawn vs the actual amount of LNFIII-DAP on the slide, which was calculated from a. The fitted curve showed linear concentration dependence
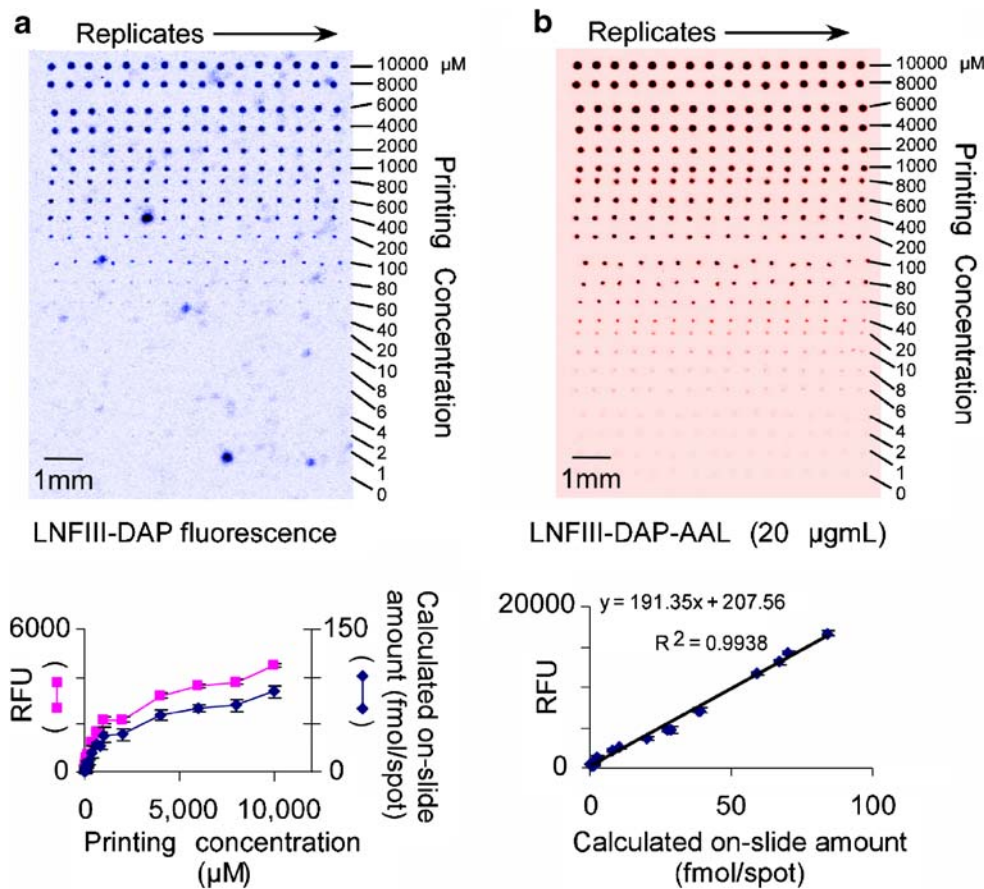
significant overlap or interference with the fluorescence of the detecting lectin or reagent that is read at a higher excitation wavelength. The results shown in Fig. 7b show that binding of AAL to LNFIII-DAP is detectable at a printing concentration of 6 μM. This level of detectability of lectin binding *vs* the concentration of printed ligand is comparable to that observed with the results in Fig. 2 and illustrate that the detectability is in the same range as that using the alternative non-fluorescent bi-functional 2-amino-methyl *N,O*-hydroxyethyl spacer [3].

An interesting feature of slide microarrays is that subarrays can be prepared on a single slide and separated from each other by a 16-chamber adaptor. This separation allowed us to examine the binding of different concentrations of AAL to the LNFIII-DAP on a single slide (Fig. 8a). We analyzed the binding of AAL from 0.01 to 20 μg/ml. There was a linear relationship between the calculated on-slide amount of LNFIII-DAP and the RFUs from the bound lectin at constant lectin concentrations (Fig. 8b). These results demonstrate that all the on-slide concentrations of LNFIII-DAP were within the linear range of LNFIII-AAL binding.

Using this data we could calculate the dose-dependent relationship between the RFU and lectin (AAL) concentration at constant LNFIII-DAP concentrations on the slide. These results (Fig. 8c) show that the binding isotherms for AAL at different LNFIII-DAP concentrations are saturable and cover the whole dynamic range of LNFIII-AAL binding. The apparent K_d for AAL binding can be easily estimated from the fitted equation using the concentration of lectin at half maximal binding at any of the glycan concentrations (Fig. 8c). Assuming a size of 33,398 Da for the monomers of the tetrameric and tetravalent AAL [6], we calculated that the apparent K_d is approximately 22 nM or 0.74 μg/ml. These results suggest a high affinity (or high avidity) binding of AAL to the immobilized LNFIII-DAP.

The multivalency of protein–carbohydrate binding on glass surface is known to affect the dissociation of lectin and its coupling partner and is commonly referred to as an increase in avidity. To determine if the glycan display on the microarray is multivalent, we explored the solution binding of AAL to LNFIII using fluorescence polarization techniques. To prepare a fluorescent derivative with high

Fig. 8 A detailed binding assay of LNFIII-DAP and AAL. a 12 replicated subarrays of decreasing LNFIII-DAP concentrations were printed as shown for a single subarray in Fig. 7 and separated by an incubation chamber. A series of AAL concentrations (20 to 0.01 μg/ml) was added separately to each incubation chamber. b The binding curve of RFU vs calculated actual on-slide amount of LNFIII-DAP at constant AAL concentration. Five curves corresponding to five AAL concentrations were merged in the same chart. c The binding curve of RFU vs AAL concentrations at constant calculated actual on-slide amount of LNFIII-DAP. Seven curves corresponding to seven LNFIII-DAP on-slide concentrations were merged in the same chart
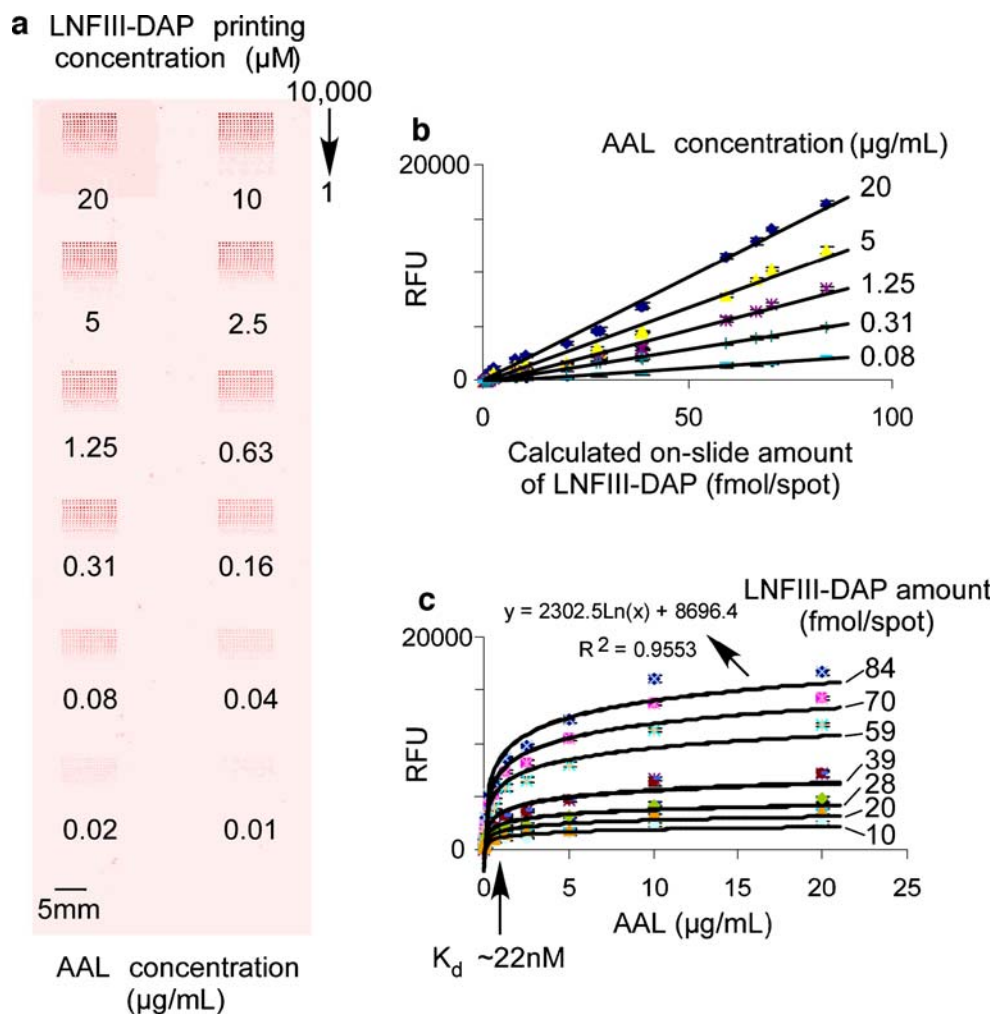
fluorescent yield in the desired wavelength, LNFIII was conjugated with ethylenediamine by reductive amination followed by conjugation with fluorescein isothiocyanate (FITC) (Fig. 9a). The concentration of LNFIII-FITC was maintained at 2 nM to provide a reasonable signal while the fluorescence polarization was measured at different AAL concentrations (from 10 ng/ml to 5 mg/ml). As a control, and to validate this approach, we examined the binding of the tetrameric, tetravalent plant lectin RCA-I to a FITC-derivative of the hexasaccharide LNnH (Fig. 9a). The binding of RCA-I to LNnH-FITC was saturable with an apparent K_d approximately 3.3 µM or 0.1 mg/ml (assuming a size of approximately 30 K_d for the monomers of RCA-I) [16] (Fig. 9b). This is in reasonable agreement with earlier determinations of RCA-I affinity for galactosylated ligands in solution [1]. As can be seen in Fig. 9c, the binding curve for the tetravalent and tetrameric AAL binding to LNFIII-FITC is not saturable and indicates that the apparent K_d for this interaction is above 2.5 mg/ml or >0.07 mM. In previous studies [12] on the inhibition of precipitation of a meconium substance with AAL by several fucose-containing sugars, it was found that the half-maximal inhibition concentrations were in the mM range [12], which is consistent with our fluorescence polarization data. Thus, the apparent dissociation in solution (mM range) is approximately five orders of magnitude higher than the K_d value of approximately 22 nM obtained from the GDAP microarray (Fig. 8c). The most reasonable interpretation of these data is that the GDAP microarray presents glycans in a high density, multivalent manner that generates high avidity binding sites for multivalent lectins. This also provides evidence that microarrays based on GDAP technology are able to detect weak protein–carbohydrate interactions.

Discussion

The development of glycan microarrays has had a profound influence on our understanding of glycan functions through the identification of specific recognition by a wide variety of glycan binding proteins from human and animal cells, in addition to viruses and bacteria [9, 18, 21, 24]. However, an important limitation in glycan array construction is the difficulty in obtaining free glycans for derivatization and quantification and the identification of printed glycans on the microarray. While chemical and semi-synthetic methods are useful, they are costly and limited to relatively small-sized glycans. Currently this approach is not really practical when considering the large size and complexity of the individual glycans of animal glycomes. The development of methods to conjugate free, reducing glycans to generate derivatives for further coupling is important, since this allows the preparation of what may be called "natural glycan arrays", consisting of free glycans found in nature or prepared directly from natural products.

There are several methods available for derivatizing free glycans to generate derivatives that have primary sulfhydryls or amines for further coupling [3], including our strategy with 2,6-diaminopyridine (DAP) [25]. A key advantage of the DAP approach, however, is that fluorescently-labeled glycans are prepared that may be easily quantified and separated from free, underivatized glycans due to the hydrophobic nature of DAP. Although this method requires reductive amination that can result in loss of structural information at the reducing end of the free glycans, it should be recognized that the primary determinants for glycan recognition in most cases are sugar residues at the non-reducing terminus. Another advantage

Fig. 9 The binding assay of LNFIII-FITC and AAL by fluorescence polarization. a The conjugation of LNFIII with FITC. b The binding assay of LNnH-FITC and RCA I as a control; a K_d can be estimated from the binding curve. c The binding curve of LNFIII-FITC and AAL. It can be estimated that the K_d is higher than 2.5 mg/ml

of the DAP method, as we show here, is that the coupled GDAPs have an enhanced fluorescence, which permits their quantification and positioning directly on printed glycan microarrays using a commonly available fluorescent slide scanner.

In the practice of data collection and analysis from microarray images in most cases, the grid localization is always difficult to achieve, due to slight and inherent irregularities of spot location. The prevailing solution is to incorporate markers at certain positions, which frequently fails at more difficult situations, such as low quality printing and weak assay signals. The GDAP microarray overcomes this problem due to the inherent fluorescence of the coupled GDAPs. For the above glycan microarray, images in Fig. 5b could be overlaid with the assayed image for easy grid localization, facilitating precise data collection, while not affecting signals from labeled proteins due to the low level of fluorescence of the background GDAP. The approach using epoxy slides permits relatively high efficiency coupling of glycans, and the use of the non-contact piezo electric printing technique permits quantification of the deposited material since, unlike contact printing methods, exact volumes (333 pl) of glycan solutions may be printed with intra tip precision of <2.5% and inter tip precision of <5.0%. It was recently reported that GDAPs do not efficiently couple to NHS-derivatized slides, based on the comparatively poor recognition by RCA-I of a single DAP derivative of the tetrasaccharide Galβ4GlcNAcβ3Galβ4Glc [3]. Here we report that the coupling efficiency of GDAPs to epoxy slides is in the range of 30–45%, while that to NHS slides is about one-fourth of that seen for coupling to epoxy slides or in the range of 5–10%. The coupling efficiency of non-fluorescent linkers as developed by others is not known, since there is no available technology to define the amount of on-slide material [2, 3, 5, 8, 11, 18, 23]. Overall, our results show that GDAP reactivity with NHS-derivatized slides is acceptable, but the more robust coupling of GDAPs to epoxy slides argues for using this coupling strategy in our studies involving coupling with DAP conjugates. In addition, epoxy slides have the advantage that epoxy is a more stable functional coupler that can be stored at room temperature and has low reactivity with water with the additional advantage that it can also react with other functional groups including free thiols [19].

Materials and methods

Free reducing glycans were purchased from V-labs and stored at −20°C until being used. All chemicals were purchased from Sigma-Aldrich and used without further purification. HPLC solvents were purchased from Fisher Scientific.

DAP conjugation of free reducing glycans

The procedure is essentially the same as described by Xia *et. al.* [25] with slight modification. A solution of 0.35 M 2,6-diaminopyridine and 1 M sodium cyanoborohydride in dimethyl sulfoxide/ acetic acid (7/3 *v/v*) was freshly prepared. To every reducing glycan (1–10 nmol), 10 μl the above solution was added, and the mixture was incubated at 65°C for 2.5 h and evaporated to dryness. The residue was dissolved in 10 μl water and applied to a GlycoClean glass cartridge (Glyko, San Leandro, CA) fitted with two pieces of 3 MM filter paper (*d*=0.5 cm). After 20 min, the cartridge was washed with 5×0.1 ml acetonitrile. The DAP conjugates, which had been absorbed to the paper and washed with acetonitrile were subsequently eluted with 3×0.5 ml water, evaporated to dryness, dissolved in 20 μl water and further purified by HPLC. No loss of sialic acid or other labile subsistent groups such as sulfate are removed by this procedure.

High performance liquid chromatography

A Shimazu HPLC CBM-20A system was used for HPLC analysis and separation of GDAPs. It is coupled with a UV detector SPD-20A and a fluorescence detector RF-10Axl. UV absorption at 330 nm or fluorescence at 330 nm excitation and 400 nm emission was used to detected GDAPs in HPLC analysis and separation. Both UV absorption and fluorescence intensity were used for the quantification of GDAPs in the solution with lactose-DAP conjugate as a standard. The fluorescence property of GDAPs at Alexa488 setting (excitation 495 nm, emission 520 nm) was also tested by HPLC using the Alexa488 setting on the fluorescence detector.

For normal phase HPLC separation, a Zorbax NH_2 column (250×4.6 mm) was used. The mobile is acetonitrile, water and 250 mM ammonium acetate (pH 4.5). The concentration of water increased from 16% to 40% over 20 min. The concentration of ammonium acetate buffer increased from 4% to 50% over 20 min. For reverse phase HPLC, a porous graphitized carbon (PGC) column (150× 4.6 mm) from Thermo was used. The mobile phase is acetonitrile and water with 0.05% trifluoroacetic acid (TFA). The concentration of acetonitrile increased from 0% to 70% over 35 min.

Printing, binding assay and scanning

Non-contact printing was performed using a Piezorray printer from Perkin Elmer. The average spot volume is within 10% variation of 1/3 nl. All the samples were printed in 1x PBS (from Fisher Bioreagents containing 11.9 mM phosphate salts, 137 mM NaCl and 2.7 mM KCl) buffer at

pH 7.4 if not described elsewhere. After printing, the slides were boxed loosely and put in a high moisture chamber at 50°C (a heated water bath works well) and incubated for 12 h. The slides were then washed and blocked with 50 mM ethanolamine in 0.1 M Tris buffer (pH 9.0) for 1 h. The slides can be dried by centrifugation and stored desiccated at −20°C for future use. Before assay, the slides were rehydrated for 5 min in TSM buffer (20 mM Tris–HCL, 150 mM NaCl, 0.2 mM $CaCl_2$ and 0.2 mM $MgCl_2$). Biotinylated lectins were used in the binding assay, and the bound lectins were detected by a secondary incubation with cyanine-5 streptavidin. For multi-panel experiment on a single slide, the array layout was designed using Piezorray software according to the dimension of a standard 16-chamber adaptor. The adaptor was applied on the slide to separate a single slide to 16 chambers sealed from each other during the assay.

The slides were scanned with a Perkin Elmer ProScanarray microarray scanner equipped with 4 lasers covering an excitation range from 488 to 637 nm. The scanned images were analyzed with the ScanArray Express software. Different excitation and emission wavelengths were used for different fluorophores. For GDAP fluorescence, 495 nm (excitation) and 520 nm (emission) were used; for cyanine-5, 649 nm (excitation) and 670 nm (emission) were used. All the images obtained from the scanner are in grayscale. For easy discrimination, the GDAP fluorescence images are shown in blue color and the cyanine-5 fluorescence images are shown in red color.

References

1. Baenziger, J.U., Fiete, D.: Structural determinants of Ricinus communis agglutinin and toxin specificity for oligosaccharides. J. Biol. Chem. **254**, 9795–9799 (1979)
2. Blixt, O., Head, S., Mondala, T., Scanlan, C., Huflejt, M.E., Alvarez, R., Bryan, M.C., Fazio, F., Calarese, D., Stevens, J., Razi, N., Stevens, D.J., Skehel, J.J., van Die, I., Burton, D.R., Wilson, I.A., Cummings, R., Bovin, N., Wong, C.-H., Paulson, J.C.: Printed covalent glycan array for ligand profiling of diverse glycan binding proteins. Proc. Natl. Acad. Sci. U. S. A. **101**, 17033–17038 (2004)
3. Bohorov, O., Andersson-Sand, H., Hoffmann, J., Blixt, O.: Arraying glycomics: a novel bi-functional spacer for one-step microscale derivatization of free reducing glycans. Glycobiology. **16**, 21C–27C (2006)
4. Cummings, R.D.: Use of lectins in analysis of glycoconjugates. Methods Enzymol. **230**, 66–86 (1994)
5. de Paz, J.L., Seeberger, P.H.: Recent advances in carbohydrate microarrays. QSAR Comb. Sci. **25**, 1027–1032 (2006)
6. Debray, H., Montreuil, J.: Aleuria aurantia agglutinin. A new isolation procedure and further study of its specificity towards various glycopeptides and oligosaccharides. Carbohydr. Res. **185**, 15–26 (1989)
7. Drickamer, K., Taylor, M.E.: Glycan arrays for functional glycomics. GenomeBiology.com **3**, reviews1034.1–reviews1034.4 (2002)
8. Feizi, T., Chai, W.: Innovation: Oligosaccharide microarrays to decipher the glyco code. Nat. Rev. Mol. Cell Biol. **5**, 582–588 (2004)
9. Feizi, T., Fazio, F., Chai, W., Wong, C.H.: Carbohydrate microarrays—a new set of technologies at the frontiers of glycomics. Curr. Opin. Struct. Biol. **13**, 637–645 (2003)
10. Fukuda, M.: Roles of mucin-type O-glycans in cell adhesion. Biochim. Biophys. Acta (G). **1573**, 394–405 (2002)
11. Hirabayashi, J.: Oligosaccharide microarrays for glycomics. Trends Biotechnol. **21**, 141–143; discussion 143 (2003)
12. Kochibe, N., Furukawa, K.: Purification and properties of a novel fucose-specific hemagglutinin of Aleuria aurantia. Biochemistry. **19**, 2841–2846 (1980)
13. Lowe, J.B.: Glycan-dependent leukocyte adhesion and recruitment in inflammation. Curr. Opin. Cell Biol. **15**, 531–538 (2003)
14. Mahajan, S., Kumar, P., Gupta, K.C.: Oligonucleotide microarrays: immobilization of phosphorylated oligonucleotides on epoxylated surface. Bioconjug. Chem. **17**, 1184–1189 (2006)
15. Merkle, R.K., Cummings, R.D.: Lectin affinity chromatography of glycopeptides. Methods Enzymol. **138**, 232–259 (1987)
16. Nicolson, G.L., Blaustein, J., Etzler, M.E.: Characterization of two plant lectins from Ricinus communis and their quantitative interaction with a murine lymphoma. Biochemistry. **13**, 196–204 (1974)
17. Ohtsubo, K., Marth, J.D.: Glycosylation in cellular mechanisms of health and disease. Cell. **126**, 855–867 (2006)
18. Paulson, J.C., Blixt, O., Collins, B.E.: Sweet spots in functional glycomics. Nat. Chem. Biol. **2**, 238–248 (2006)
19. Piehler, J., Brecht, A., Valiokas, R., Liedberg, B., Gauglitz, G.: A high-density poly(ethylene glycol) polymer brush for immobilization on glass-type surfaces. Biosens. Bioelectron. **15**, 473–481 (2000)
20. Preininger, C., Sauer, U., Dayteg, J., Pichler, R.: Optimizing processing parameters for signal enhancement of oligonucleotide and protein arrays on ARChip epoxy. Bioelectrochemistry. **67**, 155–162 (2005)
21. Raman, R., Raguram, S., Venkataraman, G., Paulson, J.C., Sasisekharan, R.: Glycomics: an integrated systems approach to structure–function relationships of glycans. Nat. Methods. **2**, 817–824 (2005)
22. Shriver, Z., Raguram, S., Sasisekharan, R.: Glycomics: a pathway to a class of new and improved therapeutics. Nat. Rev. Drug Discov. **3**, 863–873 (2004)
23. Stevens, J., Blixt, O., Paulson, J.C., Wilson, I.A.: Glycan microarray technologies: tools to survey host specificity of influenza viruses. Nat. Rev. Microbiol. **4**, 857–864 (2006)
24. Timmer, M.S., Stocker, B.L., Seeberger, P.H.: Probing glycomics. Curr. Opin. Chem. Biol. **11**, 59–65 (2007)
25. Xia, B., Kawar, Z.S., Ju, T., Alvarez, R.A., Sachdev, G.P., Cummings, R.D.: Versatile fluorescent derivatization of glycans for glycomic analysis. Nat. Methods. **2**, 845–850 (2005)
26. Yamamoto, K., Tsuji, T., Osawa, T.: Analysis of asparagine-linked oligosaccharides by sequential lectin-affinity chromatography. Methods Mol. Biol. **76**, 35–51 (1998)
27. Yamashita, K., Kochibe, N., Ohkura, T., Ueda, I., Kobata, A.: Fractionation of L-fucose-containing oligosaccharides on immobilized Aleuria aurantia lectin. J. Biol. Chem. **260**, 4688–4693 (1985)